

# Asymptotic Expansions and Amplification of a Gravitational Lens Near a Fold Caustic

A.N. Alexandrov<sup>1</sup> \* and V.I. Zhdanov<sup>1,2</sup> †

<sup>1</sup> *Astronomical Observatory, Taras Shevchenko National University of Kyiv, 3, Observatorna Str., Kyiv 04053, Ukraine*

<sup>2</sup> *National Technical University of Ukraine “Kyiv Polytechnic Institute”, Kyiv 03056, Ukraine*

Accepted 2011 June 21. Received 2011 May 25; in original form 2010 July 14

## ABSTRACT

We propose two methods that enable us to obtain approximate solutions of the lens equation near a fold caustic with an arbitrary degree of accuracy. We obtain “post-linear” corrections to the well-known formula in the linear caustic approximation for the total amplification of two critical images of a point source. In this case, in order to obtain the nontrivial corrections we had to go beyond the approximation orders earlier used by Keeton et al. and to take into account the Taylor expansion of the lens equation near caustic up to the fourth order. Corresponding analytical expressions are derived for the amplification in cases of the Gaussian and power-law extended source models; the amplifications depend on three additional fitting parameters. Conditions of neglecting the correction terms are analysed. The modified formula for the amplification is applied to the fitting of light curves of the Q2237+0305 gravitational lens system in a vicinity of the high amplification events (HAEs). We show that the introduction of some “post-linear” corrections reduces  $\chi^2$  by 30 per cent in the case of known HAE on the light curve of image C (1999). These corrections can be important for a precise comparison of different source models with regard for observational data.

**Key words:** gravitational lensing: micro – quasars: individual (Q2237+0305) – gravitational lensing: strong – methods: analytical

## 1 INTRODUCTION

An extragalactic gravitational lens system (GLS) forms several images of a single quasar. The light from the quasar intersects a lensing galaxy in different regions which correspond to different images. Variations of gravitational fields in these regions due to stellar motions are practically independent and lead to independent brightness variations in different images (gravitational microlensing). Comparison of the light curves of different images allows one to obtain a valuable information about the lens itself and about the source as well (Schneider, Ehlers & Falco 1992; Wambsganss 2006). One of the important applications of this effect deals with a unique possibility to study a fine structure of the central quasar region with the use of GLS. This idea first proposed by Grieger, Kayser & Refsdal (1988) appeals to the high amplification events (HAEs) in one of the images of the quasar in GLS. An interesting applications of HAEs are known also in Galactic microlensing (see, e.g. Wambsganss 2006), in particular, using the caustic crossing events for resolving of stellar profiles (Bogdanov & Cherepashchuk 2002; Dominik 2004).

The conventional explanation of HAE relates it to the caustic field in the source plane formed due to the inhomogeneous gravitational field of a lensing galaxy on the line of sight of the image (Schneider et al. 1992). The source crossing of a caustic leads to a considerable enhancement of the image brightness, the crossing of a fold caustic being the most probable. The corresponding variations of the brightness in a neighborhood of HAE can be approximately described by a formula containing a few fitting parameters. This makes it possible to estimate certain HAE characteristics, in particular, such as the source size (Grieger et al. 1988). For example, in the case of the well-known Q2237+0305 GLS (Einstein Cross), several HAEs was

\* E-mail: alex@observ.univ.kiev.ua

† E-mail: ValeryZhdanov@mail.ru

observed (Wozniak et al. 2000; Alcalde et al. 2002; Udalski et al. 2006), and the estimates of the source size have been obtained within different source models (Wyithe, Webster & Turner 1999, 2000; Wyithe et al. 2000; Yonehara 2001; Shalyapin 2001; Shalyapin et al. 2002; Bogdanov & Cherepashchuk 2002). Almost all HAEs in the Q2237+0305 GLS are attributed just to a fold caustic crossing in the source plane (see, e.g., Gil-Merino et al. 2006). A possibility to distinguish different source models is also discussed (e.g. Goicoechea et al. 2003).

The lens equation near a fold can be expanded in powers of local coordinates; in the lowest orders of this expansion, the caustic is represented by a straight line; so, this approximation is often referred as a “linear caustic approximation”. In this approximation, the point source flux amplification is given by a simple formula, which depends on the distance to the caustic and contains two parameters (e.g. Schneider et al. 1992, Cassan 2008). In most cases, the linear caustic approximation is sufficient to fit the observed light curves over the range of HAEs at the modern accuracy of flux measurements. The need for a modification of this formula – e.g., by taking the caustic curvature into account – is, nevertheless, being discussed for a long time (Fluke & Webster 1999; Shalyapin 2001; Pejcha & Heyrovský 2009). We hope that the future improvement of the photometric accuracy will make it possible to obtain additional parameters of the lens mapping, which are connected with the mass distribution in the lensing galaxy. At the same time, we will show that the consideration of “post-linear” terms is sometimes appropriate to explain the present observational data. We note that the corrections to the amplification factor in the case of macrolensing were the subject of investigations dealing with the problem of “anomalous flux ratios” (Keeton, Gaudi & Petters 2005).

Since the work by Kochanek (2004) followed by a number of works (Mortonson, Schechter & Wambsganss 2005; Gil-Merino et al. 2006; Vakulik et al. 2007; Anguita et al. 2008; Poindexter, Morgan & Kochanek 2008; Poindexter & Kochanek 2010a,b), numerous statistical methods have been developed to process complete light curves. This approach is very attractive because it allows one to consider the whole aggregate of observational data on image brightness variations in order to estimate the microlens masses and the source model parameters. However, this treatment involves a large number of realizations of the microlensing field, which requires a considerable computer time. On the other hand, the source structure manifests itself only in HAEs; far from the caustic, the source looks like a point one, and all the information about its structure is lost. If we restrict ourselves to the HAE neighborhood, then we use the most general model concerning a microlensing field described by a small collection of Taylor coefficients in the lens mapping. Therefore, the low-time-consuming semi-analytical investigations dealing with caustic neighborhoods still preserve their importance, not speaking about their use in computer codes.

In this paper, we propose relations for the total magnification of two critical images of a point source in the first nontrivial “post-linear” approximations and use them to modify the magnification of an extended source near the fold caustic. In order to obtain non-zero corrections to the total amplification of two critical images, we have to consider additional higher-order terms in the expansion of the lens mapping in comparison with the earlier works (see, e.g., Keeton et al. 2005). Though the corrections are expected to be small, they appear to be noticeable in some cases even in an analysis of the existing data on light curves in the Q2237+0305 GLS. The structure of this paper is as follows: after the derivation of approximate solutions of the lens equation in the required order, we deduce a formula for the magnification of a point source. The result is used to obtain the magnification of a small Gaussian source near the fold caustic. We use the formula for the amplification of an extended source to fit the light curves in GLS Q2237+0305. The obtained post-linear corrections appear to improve the agreement with observational data.

Appendices A and B contain details on the approximation methods involved. Power-law source models are considered in Appendix C. Explicit comparison of our approximate formulas with counterparts from the paper by Keeton et al. (2005) is made in Appendix D.

## 2 INITIAL EQUATIONS

First, we recall some general notions concerning the gravitational lensing that can be found, e.g., in the book by Schneider et al. (1992). The normalized lens equation has the form:

$$\mathbf{y} = \mathbf{x} - \nabla\Phi(\mathbf{x}), \quad (1)$$

where  $\Phi(\mathbf{x})$  is the lens potential. This equation relates every point  $\mathbf{x} = (x_1, x_2)$  of the image plane to the point  $\mathbf{y} = (y_1, y_2)$  of the source plane. In the general case, there are several solutions  $\mathbf{X}_{(i)}(\mathbf{y})$  of the lens equation (1) that represent images of one point source at  $\mathbf{y}$ ; we denote the solution number by the index in parentheses.

If there is no continuous matter on the line of sight, the potential must be a harmonic function  $\Delta\Phi = 0$ . Below, we will assume that this condition is fulfilled in a neighborhood of the critical point. We note, however, that if the continuous matter density is supposedly constant during HAE, this can be taken into account by a suitable rescaling of the variables.

The amplification of a separate image of a point source is

$$K_{(i)}(\mathbf{y}) = 1/|J(\mathbf{X}_{(i)}(\mathbf{y}))|, \quad (2)$$

where  $J(\mathbf{x}) \equiv |D(\mathbf{y})/D(\mathbf{x})|$  is the Jacobian of the lens mapping. In the microlensing processes, microimages cannot be observed separately; therefore, we need the total amplification which is a sum of the amplification coefficients of all the images.

The critical curves of the lens mapping (1) are determined by the equation  $J(\mathbf{x}) = 0$  and are mapped onto the caustics in the source plane. The stable critical points of a two-dimensional mapping can be folds and cusps only, the folds being more probable in HAE. In this paper, we confine ourselves to the consideration of fold caustics. When a point source approaches the fold caustic from its convex side, two of its images approach the critical curve, and their magnification tends to infinity. They disappear when the source crosses the caustic. These two images are called critical.

The standard consideration of the caustic crossing events deals with the Taylor expansion of the potential near some point  $p_{cr}$  of the critical curve in the image plane. Let this point be the coordinate origin. We suppose that (1) maps  $p_{cr}$  onto the coordinate origin of the source plane. Further, we rotate synchronously the coordinate systems until the abscissa axis on the source plane be tangent to the caustic at the origin. The quantity  $|y_2|$  defines locally the distance to the caustic, and  $y_1$  defines a displacement along the tangent. For the harmonic potential, we can write

$$\begin{aligned} y_1 &= 2x_1 + a(x_1^2 - x_2^2) + 2bx_1x_2 + c(x_1^3 - 3x_1x_2^2) - d(x_2^3 - 3x_2x_1^2) + gx_2^4 + \dots, \\ y_2 &= b(x_1^2 - x_2^2) - 2ax_1x_2 + d(x_1^3 - 3x_1x_2^2) + c(x_2^3 - 3x_2x_1^2) + fx_2^4 + \dots, \end{aligned} \quad (3)$$

where  $a, b, c, d, g,$  and  $f$  are expansion coefficients. If the  $y_2$  axis is directed toward the convexity of the caustic, then  $b < 0$  (at fold points,  $b \neq 0$ ).

### 3 EXPANSION OF THE CRITICAL SOLUTIONS IN POWERS OF A SMALL PARAMETER

#### 3.1 Method 1

We now proceed to the derivation of approximate solutions of Eqs. (3). To do this, we present two different methods which will be used to have a possibility of mutual checks of cumbersome calculations. The first method deals with analytical expansions in powers of a small parameter. However, it results in nonanalytic functions of coordinates leading to nonintegrable terms in the amplification factor. The second method does not lead to such problems, though it uses a somewhat more complicated representation of the solution of the lens equation (containing square roots of analytic functions). The methods agree with each other in a common domain of validity; moreover, we use the second method to justify some expressions in the amplification formulas in terms of distributions to validate applications to extended source models.

First, we use a regular procedure proposed by Alexandrov, Zhdanov & Fedorova (2003) to construct solutions of Eqs. (3) with a desired accuracy. This procedure is useful to study the light curve of the point source which has a trajectory crossing the fold caustic at some nonzero angle. We suppose that the source and the caustic lie on different sides from the  $y_1$  axis. Then, for  $y_2 > 0$ , we substitute

$$y_i = t^2 \tilde{y}_i, \quad x_1 = t^2 \tilde{x}_1, \quad x_2 = t \tilde{x}_2, \quad (4)$$

where  $i = 1, 2$ , and  $t$  can be considered as a parameter of vicinity to the caustic. This is a formal substitution that makes easier operations with different orders of the expansion. After performing calculations, we shall put  $t = 1$  and thus return to the initial variables  $y_i$ . However, if we put  $\tilde{y}_i$  to be constant with varying  $t$ , then this substitution allows us to study a local behaviour of critical image trajectories;  $t = 0$  corresponds to crossing the caustic by a point source, and  $t^2$  can be considered as the time counted from the moment, when two critical images appear. Indeed, one can show (Alexandrov et al. 2003) that two critical solutions  $\mathbf{X}_i(t) = (X_{(i)1}, X_{(i)2})$  of the lens equation can be represented by analytic functions of  $t$  that, in the above special coordinate system, have the behaviour  $X_{(i)1} \propto t^2$ ,  $X_{(i)2} \propto t$  (see Appendix A). This allows us to look for solutions of Eqs. (3), by using the expansions of  $\tilde{x}_i$  in powers of  $t$ :

$$\begin{aligned} \tilde{x}_1 &= \tilde{x}_{10} + \tilde{x}_{11}t + \tilde{x}_{12}t^2 + \dots, \\ \tilde{x}_2 &= \tilde{x}_{20} + \tilde{x}_{21}t + \tilde{x}_{22}t^2 + \dots \end{aligned} \quad (5)$$

It should be stressed that the analyticity in  $t$  does not mean that the coefficients of expansions (5) will be analytic functions of coordinates  $\tilde{y}_i$  in the source plane (see below).

In terms of the new variables (4), system (3) takes the form (up to the terms  $\sim t^2$ )

$$\begin{aligned} \tilde{y}_1 &= 2\tilde{x}_1 - a\tilde{x}_2^2 + t(2b\tilde{x}_1\tilde{x}_2 - d\tilde{x}_2^3) + t^2(a\tilde{x}_1^2 - 3c\tilde{x}_1\tilde{x}_2^2 + g\tilde{x}_2^4), \\ \tilde{y}_2 &= -b\tilde{x}_2^2 + t(-2a\tilde{x}_1\tilde{x}_2 + c\tilde{x}_2^3) + t^2(b\tilde{x}_1^2 - 3d\tilde{x}_1\tilde{x}_2^2 + f\tilde{x}_2^4). \end{aligned} \quad (6)$$

The substitution of expansions (5) into (6) allows us to determine all coefficients successively. The results of calculations are as follows.

For the zero-order terms:

$$\tilde{x}_{10} = \frac{1}{2} \left( \tilde{y}_1 - \frac{a}{b} \tilde{y}_2 \right), \quad \tilde{x}_{20} = \varepsilon \sqrt{\tilde{y}_2 / |b|}, \quad (7)$$

where  $\varepsilon = \pm 1$  determines two different solutions.

The first-order terms are

$$\tilde{x}_{11} = -\varepsilon \sqrt{\frac{\tilde{y}_2}{|b|}} \frac{(ac - aR^2 + bd) \tilde{y}_2 + bR^2 \tilde{y}_1}{2b^2}, \quad \tilde{x}_{21} = \frac{1}{2} \left( \frac{a^2 - c}{b^2} \tilde{y}_2 - \frac{a}{b} \tilde{y}_1 \right), \quad (8)$$

where  $R^2 = a^2 + b^2$ . The solutions up to this accuracy has been obtained earlier by Alexandrov et al. (2003) and Keeton et al. (2005) (see also Congdon, Keeton & Nordgren (2008)). The contributions of this order are cancelled in calculations of the total amplification factor of two critical images. Therefore, to obtain a nontrivial correction to the zero-order amplification, higher order approximations should be involved.

The second-order terms contain an expression nonanalytical in  $\tilde{y}_2$ :

$$\tilde{x}_{12} = \frac{1}{4b^4} (3a^5 + 5a^3b^2 + 2ab^4 - 2b^3d - 2b^2g + 3ac^2 - 6a^3c + 3bcd - 8a^2bd + 2abf) \tilde{y}_2^2 + \frac{1}{2b^3} (2a^2c - b^2c + 3abd - 2a^2R^2 - b^2R^2) \tilde{y}_1 \tilde{y}_2 + \frac{aR^2}{4b^2} \tilde{y}_1^2, \quad (9)$$

$$\tilde{x}_{22} = \varepsilon \sqrt{\frac{\tilde{y}_2}{|b|}} \left[ \frac{1}{8b^3} (10a^2c - 5c^2 - 5a^2R^2 + 10abd - 4bf) \tilde{y}_2 - \frac{3}{4b^2} (ac + bd - aR^2) \tilde{y}_1 - \frac{R^2}{8b} \frac{\tilde{y}_1^2}{\tilde{y}_2} \right]. \quad (10)$$

### 3.2 Method 2

The second approach to the construction of approximate solutions of the lens equation in a vicinity of the fold is described in Appendix B. This allows us to provide the critical solutions of system (6) in the following form:

$$\tilde{x}_1 = p + t\varepsilon\sqrt{w}, \quad \tilde{x}_2 = t\bar{s} + \varepsilon\sqrt{w}, \quad \varepsilon = \pm 1. \quad (11)$$

The iterative procedure described in Appendix B yields analytical expansions for the functions  $p, r, \bar{s}, w$  both in powers of  $t$  and  $\tilde{y}_i$ . The application of this method to system (6) gives (up to the terms  $\sim t^2$ )

$$p = \tilde{x}_{10} + t^2 \tilde{x}_{12}, \quad (12)$$

where  $\tilde{x}_{10}$  and  $\tilde{x}_{12}$  are given by relations (7) and (9), and

$$r = -\frac{R^2 \tilde{y}_1}{2b} + \frac{\tilde{y}_2}{2b^2} [aR^2 - (ac + bd)], \quad \bar{s} = -\frac{a}{2b} \tilde{y}_1 + \frac{a^2 - c}{2b^2} \tilde{y}_2, \quad (13)$$

$$w = -\frac{\tilde{y}_2}{b} + \frac{t^2}{4b^2} \left[ R^2 \tilde{y}_1^2 + \frac{6}{b} (bd - ab^2 + ac - a^3) \tilde{y}_1 \tilde{y}_2 + \frac{1}{b^2} (5a^2(R^2 - 2c) + 5c^2 - 10abd + 4bf) \tilde{y}_2^2 \right]. \quad (14)$$

As is seen, all these expressions are analytic functions of both  $t$  and  $\tilde{y}_i$ . If we expand  $\sqrt{w}$  in powers of  $t$ , then we immediately have the solution in the form (5) with coefficients (7), (8), (9), and (10).

## 4 AMPLIFICATION FACTOR

### 4.1 Point source

For the Jacobians  $J(\mathbf{X}_{(i)}(t^2 \tilde{\mathbf{y}}))$  ( $i = 1, 2$  corresponds to  $\varepsilon = \pm 1$ ), we obtain up to the terms  $\sim t^3$ :

$$J = 4\varepsilon t \sqrt{|b| \tilde{y}_2} + 4t^2 \frac{(R^2 - c)}{b} \tilde{y}_2 + \varepsilon t^3 \sqrt{|b| \tilde{y}_2} \left[ -3 \frac{a(R^2 - c) - bd}{b^2} \tilde{y}_1 + \frac{1}{2b^3} (7a^2R^2 - 8cR^2 + 7c^2 - 6a^2c - 30abd + 24b^2c + 12bf) \tilde{y}_2 - \frac{R^2}{2b} \frac{\tilde{y}_1^2}{\tilde{y}_2} \right]. \quad (15)$$

According to (2), the value of  $J^{-1}$  yields the amplification of individual images. Note that the terms up to order  $\sim t^2$  were obtained by Keeton et al. (2005). The final result for the total amplification of two critical images (in terms of the initial variables  $y_i$  after putting  $t = 1$ ) is as follows:

$$K_{cr} = \frac{1}{2} \frac{\Theta(y_2)}{\sqrt{|b| y_2}} \left[ 1 + Py_2 + Qy_1 - \frac{\kappa}{4} \frac{y_1^2}{y_2} \right], \quad (16)$$

where

$$P = 2\kappa + \frac{15}{8|b|^3} [a^2b^2 + (a^2 - c)^2] - \frac{3}{4b^2}(2f - 5ad), \quad Q = \frac{3}{4b^2} (a^3 - ac + ab^2 - bd), \quad \kappa = \frac{a^2 + b^2}{2|b|}, \quad (17)$$

$\Theta(y_2)$  is the Heaviside step function. Note that  $\kappa$  is the caustic curvature at the origin (Gaudi & Petters 2002; Alexandrov et al. 2003) which enters explicitly into the amplification formula.

Formula (16) yields an effective approximation for the point source magnification near the coordinate origin provided that  $y_2 > 0$ , and  $y_2/y_1^2$  is not too small (see the term containing  $\kappa$ ). For a fixed source position, this can be satisfied always by an appropriate choice of the coordinate origin, so that the source will be situated almost on a normal to the tangent to the caustic.

If the source is on the caustic tangent or in the region between the caustic and the tangent, then formula (16) does not represent a good approximation to the point source magnification. Nevertheless, in case of an extended source, we will show that result (16) can be used to obtain approximations to the amplification of this source even as it intersects the caustic. However, to do this, we need to redefine correctly the convolution of (16) with a brightness distribution.

## 4.2 Transition to extended source

Let  $I(\mathbf{y})$  be a surface brightness distribution of an extended source. If the source center is located at the point  $\mathbf{Y} = (Y_1, Y_2)$  in the source plane, then the total microlensed flux from the source is

$$F(\mathbf{Y}) = \iint I(\mathbf{y}(\mathbf{x}) - \mathbf{Y}) dx_1 dx_2 = \iint K(\mathbf{y}) I(\mathbf{y} - \mathbf{Y}) dy_1 dy_2, \quad (18)$$

where the point source amplification  $K(\mathbf{y}) = \sum_i K_i$  is the sum of amplifications of all the images. The result of using the first integral from Eq. (18) obviously is equivalent to the result of the well-known ray-tracing method (Schneider et al. 1992) (when the pixel sizes tend to zero). Near a caustic, one can approximate  $K(\mathbf{y}) = K_0 + K_{cr}(\mathbf{y})$ , where  $K_0$  is an amplification of all noncritical images that is supposed to be constant during HAE, and  $K_{cr}$  is the amplification of the critical images.

Formula (16) contains the non-integrable term  $\sim \Theta(y_2)(y_2)^{-3/2}$ . Therefore, the question arises of how formula (16) can be used in situation when the extended source intersects a caustic and some part of the source is in the zone between the tangent and the caustic. In view of Section 3.2, it is evident that the mentioned term is a result of the expansion of the root  $\sqrt{y_2 + \kappa y_1^2 t^2/2 + \dots}$  in the approximate solution (11-14). Any non-integrable terms in  $K_{cr}$  does not arise without using this expansion. It is easy to show that, in order to define  $K_{cr}$  correctly, one must replace the term  $\Theta(y_2)(y_2)^{-3/2}$  in (16) by the distribution (generalized function)  $(y_2)_+^{-3/2}$  (Gel'fand & Shilov 1964). We recall that the distribution  $y_+^{-3/2}$  of the variable  $y$  is defined by the expression

$$\int y_+^{-3/2} f(y) dy = \int_0^\infty \frac{f(y) - f(0)}{y^{3/2}} dy = 2 \int_0^\infty y^{-1/2} \frac{\partial f(y)}{\partial y} dy$$

for any test function  $f(y)$ .

After this redefinition, we have

$$K_{cr} = \frac{\Theta(y_2)}{2\sqrt{|b|}y_2} [1 + Py_2 + Qy_1] - \frac{\kappa}{8\sqrt{|b|}} y_1^2 (y_2)_+^{-3/2}. \quad (19)$$

This formula can be used to correctly derive an approximate magnification of a sufficiently smooth extended source including the case where the source crosses the caustic.

## 4.3 Extended Gaussian source

Now we use formula (19) to derive the magnification of a Gaussian source with the brightness distribution

$$I_G(\mathbf{y}) = \frac{1}{\pi L^2} \exp(-\mathbf{y}^2/L^2), \quad (20)$$

where the parameter  $L$  characterizes the source size.

The amplification of an extended source is defined as the ratio of the lensed flux (18) to the flux of the unlensed source  $F_0 = \iint I(\mathbf{y}) dy_1 dy_2$  which is equal to 1 in case of formula (20). The amplification of a Gaussian source  $K_G$  is obtained by the substitution of (20) and (19) into (18).

Further, we introduce the dimensionless coordinates  $s = Y_1/L$ ,  $h = Y_2/L$  of the source centre and the functions

$$I_k(h) = \int_0^\infty u^{k-1/2} \exp(-u^2 + 2uh) du = \frac{1}{2} \sum_{n=0}^\infty \frac{\Gamma(\frac{1}{4} + \frac{k+n}{2})}{n!} (2h)^n. \quad (21)$$

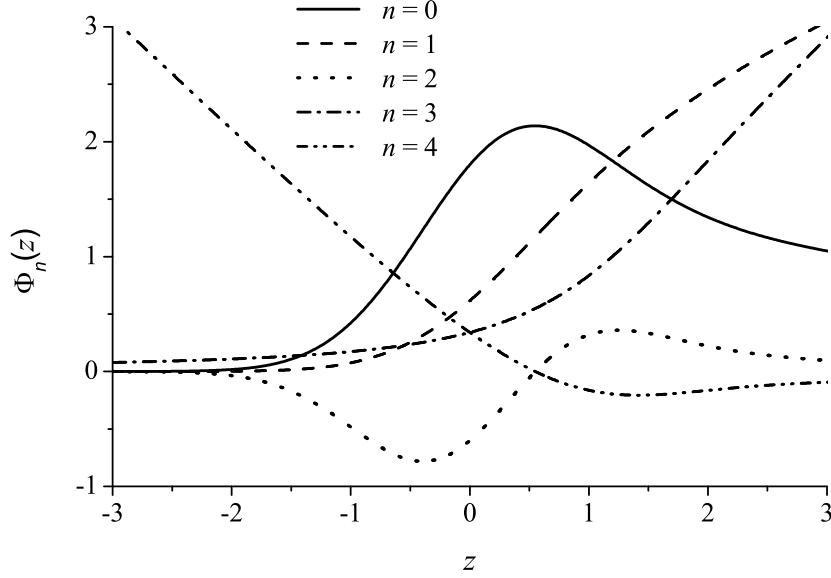


**Figure 1.** Behaviour of individual functions (24) which generate dependence (23) and the ratios (26) of correction functions to the main one.

These functions can be expressed in terms of the confluent hypergeometric function  ${}_1F_1$  or the parabolic cylinder function  $D$  (Bateman & Erdélyi 1953):

$$I_k(h) = \frac{1}{2}\Gamma\left(\frac{1}{4} + \frac{k}{2}\right) {}_1F_1\left(\frac{1}{4} + \frac{k}{2}, \frac{1}{2}; h^2\right) + h\Gamma\left(\frac{3}{4} + \frac{k}{2}\right) {}_1F_1\left(\frac{3}{4} + \frac{k}{2}, \frac{3}{2}; h^2\right) = 2^{-\left(\frac{k}{2} + \frac{1}{4}\right)}\Gamma\left(k + \frac{1}{2}\right) e^{\frac{h^2}{2}} D_{-(k+\frac{1}{2})}(-\sqrt{2} \cdot h). \quad (22)$$

The substitution of (19) and (20) in (18) yields

$$K_G(s, h) = \frac{1}{2\sqrt{\pi|b|L}} \left\{ \Phi_0(h) + L \left[ P\Phi_1(h) - \frac{\kappa}{2}\Phi_2(h) + Qs\Phi_0(h) - \kappa s^2\Phi_2(h) \right] \right\}. \quad (23)$$

Here,

$$\Phi_0(h) = I_0(h) \exp(-h^2), \quad \Phi_1(h) = I_1(h) \exp(-h^2), \quad \Phi_2(h) = [hI_0(h) - I_1(h)] \exp(-h^2). \quad (24)$$

We have checked this result by the direct substitution of expansions (6) in the first integral of Eq. (18), assuming  $t = \sqrt{L}$  and expanding the resulting integral in powers of this parameter up to the second order. Note that the main term of (23) which corresponds to the linear caustic approximation was first obtained by Schneider & Weiß (1987).

Analogous considerations allowed us to obtain formulas for the magnification of extended sources for two types of power-law brightness profiles (Appendix C); the results are represented analytically in terms of hypergeometric functions.

Let us discuss formula (23) in more details. The functions  $\Phi_i(h)$  are shown in Fig. 1. The distinctive variations of these functions take place for  $-2L < y_2 < 2L$ . For  $y_2 < -2L$ , they are practically equal to zero, and, for  $y_2 > 2L$ , they have the following asymptotic behavior:

$$\Phi_0(h) \cong \sqrt{\frac{\pi}{h}}, \quad \Phi_1(h) \cong \sqrt{\pi h}, \quad \Phi_2(h) \cong \frac{1}{4h} \sqrt{\frac{\pi}{h}}. \quad (25)$$

We also introduce the functions

$$\Phi_3(h) = \Phi_1/\Phi_0, \quad \Phi_4(h) = -\Phi_2/\Phi_0, \quad (26)$$

which are designed to estimate the contribution of the correction terms. These functions are also shown in Fig. 1. At the origin, we have  $\Phi_3(0) = \Phi_4(0) = 0.338$ .

A special attention must be given to the term which is proportional to the monotonically increasing function  $\Phi_1(h)$ . This correction becomes especially noticeable on the inner side of the caustic, its sign being determined by the sign of the parameter  $P$  from Eqs. (17). Such behaviour allows us to hope that the determination of this term from the observational data will not be too difficult.

The effect of the third term of formula (23) that is proportional to  $\Phi_2(h)$  is shown in Fig. 2 by the dependence  $\Phi_0(h) - \alpha\Phi_2(h)$  for various values of the coefficient  $\alpha$ . According to (23), the parameter  $\alpha = L\kappa/2$  equals to half of

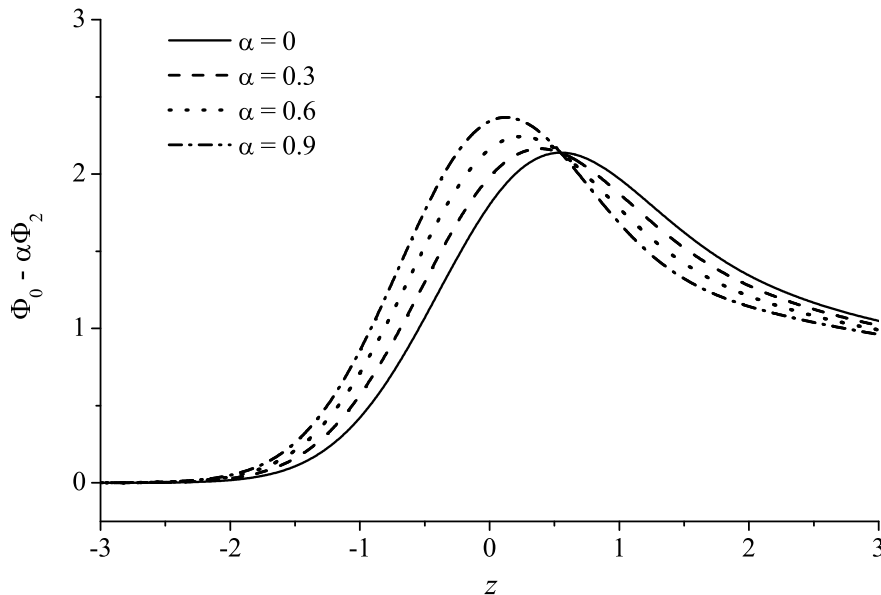


**Figure 2.** Influence of the correction term proportional to  $\Phi_2$ .

the ratio of the source radius to the curvature radius of the caustic at the origin. One can see from Fig. 2 that this term can noticeably affect the determination of the source size and the time moment of crossing the caustic .

The last two terms of Eq (23) contain  $s \propto y_1$  and  $s^2 \propto y_1^2$ . For a fixed position of the source, one can exclude these terms by the origin displacement. In case of the rectilinear motion of a source, the impact of these terms can be noticeable for small angles of the intersection of the source trajectory with the caustic.

We now discuss the conditions of applicability of the approximation methods involved for modelling the light curves in a vicinity of HAE. For example, with regard for observational data, we can require that, in the interval  $-0.5 \leq h \leq 1$ , the contribution of each correction do not exceed five per cent. We see from Fig. 1 that, in this interval,  $\Phi_3(h) < \Phi_3(1) \approx 0.83$  and  $|\Phi_4(h)| < \Phi_4(-0.5) \approx 0.73$ . From the condition of smallness of the corrections, we find the following restrictions on the parameters of the model:

$$LP < 0.06, \quad L\kappa < 0.13, \quad LQ \cdot \cot(\beta) < 0.05, \quad L\kappa \cdot \cot^2(\beta) < 0.27, \quad (27)$$

where  $\beta$  is the angle between the source trajectory and the caustic. Under these conditions and within the specified margin of error, one can use the linear caustic approximation. Thus, in addition to the requirement of the smallness of the caustic curvature, we obtain some extra restrictions on the possible variations of the lens potential on the scale of the source size. It is clear that the strengthening of requirements for the model accuracy and/or the extension of the interval of  $h$  leads to the strengthening of the conditions found.

Clearly, formulas (19) and (23) make sense only if we can ignore the discarded high-order terms. This means, in turn, that the correction terms in (23) themselves must be sufficiently small.

## 5 HAE IN THE EINSTEIN CROSS

The Einstein Cross QSO 2237+0305 (Huchra et al. 2008) consists of a quadruply imaged quasar and a lensing galaxy that is the nearest of all known gravitational lens systems ( $z_G = 0.0395$ ). The gravitational delay times between images in this GLS are of the order of hours. This follows from a highly symmetric configuration of the images and is partially confirmed by observations (see, e.g., Schmidt, Webster & Lewis 1998; Dai et al. 2003; Vakulik et al. 2006; Fedorova et al. 2008). Since the Einstein Cross is a very suitable object for microlensing studies, its images have been continuously monitored by different groups for more than a dozen of years. In this system, significant microlensing-induced brightness peaks on light curves of the quasar images were detected (see, e.g., Wozniak et al. 2000; Alcalde et al. 2002; Moreau et al. 2005).

**Fitting the light curves and estimations of HAE parameters in GLS Q2237+0305**

We now apply formula (23) to the fitting of the light curves near HAE. For a moving source,  $Y_i = V_i(t - t_C)$ , where  $t$  is the time,  $t_C$  is the time of the crossing of the caustic by the source centre,  $V_i$  is the projection of the source velocity on the axis  $y_i$ . We suppose that  $V_2 \gg V_1$ , i.e. the source crosses the caustic effectively and does not move along it. Our numerical simulations have shown that the terms depending upon the coordinate  $s$  contribute only for small angles between the source trajectory and the tangent to the caustic. Therefore, we do not take them into account, and, correspondingly, the parameter  $Q$  is not involved into consideration. Introducing the parameter  $T = L/|V_2|$ , we obtain  $h = \pm(t - t_C)/T$  (the sign “+” corresponds to the source motion along the positive direction of the  $y_2$  axis).

We consider the known HAE in the light curve of image C of GLS Q2237+0305 using the OGLE data recorded during 1999 (Wozniak et al. 2000). Let  $F_0$  be the flux from image C when the microlensing is absent. Under the supposition that the proper brightness variations of the quasar in GLS can be neglected and taking expression (23) for the amplification into account, we obtain the formula for fitting the flux from the microlensed Gaussian source,

$$F^M(t) = A + B\Phi_0(h) + C\Phi_1(h) + D\Phi_2(h), \quad (28)$$

which contains the parameters

$$A = F_0 K_0, \quad B = F_0 / \sqrt{4\pi T |b| |V_2|}, \quad C = F_0 P \sqrt{T |V_2| / 4\pi |b|}, \quad D = -\frac{1}{4} F_0 \kappa \sqrt{T |V_2| / \pi |b|},$$

and  $t_C$  and  $T$  which appear nonlinearly. The quantity  $K_0$  in the expression for  $A$  is a part of the amplification due to noncritical images. The parameters  $A$  and  $B$  are evidently positive,  $D$  is negative, and  $C$  can have values of both signs. As discussed above, the possibility to use the linear caustic approximation or formula (23) is determined by the ratios of corrections coefficients to the coefficient  $B$  of the zeroth approximation:  $C/B = LP$ ,  $D/B = -L\kappa/2$ .

To fit the light curve, we used the minimization of the weighted sum of squares:

$$S = \sum_{i=1}^N W_i [F_i - F^M(t_i)]^2, \quad (29)$$

where  $F_i$  is the result of the  $i$ -th measurement, and  $W_i = 1/\sigma_i^2$  is its weight that is expressed through the corresponding dispersion estimate  $\sigma_i$  (Wozniak et al. 2000). The fitting quality is often characterized by the parameter  $\chi^2 = S_{\min}/\nu$ ,  $\nu$  being the number of degrees of freedom. The value of this parameter in the optimal case should tend to 1.

As  $F^M$ , we have considered the following models:

$$F^0(t) = A + B\Phi_0(h),$$

$$F^1(t) = A + B\Phi_0(h) + C\Phi_1(h),$$

$$F^2(t) = A + B\Phi_0(h) + D\Phi_2(h).$$

We also analysed the model that takes both correction terms  $C\Phi_1(h) + D\Phi_2(h)$  into account. However, we found that it does not allow us to obtain the coefficients that are statistically significant simultaneously. For comparison, we also considered the model with a correction term linear in  $h$ ; such a correction can be caused by the own variability of the quasar, or by the influence of noncritical images (cf. Yonehara 2001):

$$F^3(t) = A + B\Phi_0(h) + Eh.$$

The results of best-fitting with different models are presented in Table 1. It contains the estimates of model parameters and their central 95-per-cent confidence intervals that have been found by the Monte-Carlo simulations under supposition of the normal distribution of errors. In all the models, the correction terms are statistically significant. The probability that the correction coefficient is occasionally nonzero is certainly less than  $10^{-3}$  in every case. On the other hand, all three models can compete with one another on an equal footing (and probably with another effects such as those due to a complicated source structure).

Note that the flux variation of the model light curve is roughly equal to 0.18 mJy, and the standard deviation of data is  $\sigma \approx 0.006$  mJy. Thus, the assumption of the 5-per-cent tolerance in a vicinity of the light curve maximum, which has been used in criteria (27), is rather realistic. In the case of the  $F^1$ -model, we find  $C/B = LP \approx 0.076$ . The comparison with the first inequality in (27) indicates the agreement with the statistical significance of the first correction term.

Fig. 3 shows the results of light curve fitting for image C in the region of HAE with the  $F^1$ -model. Here, 44 data points were included corresponding to the [1289,1442] epoch interval (light circles). To choose a fitting interval in a vicinity of the light curve maximum, we used the fact that the values of fitting parameters are reasonably stable with respect to a reduction of the interval. This allowed us to find a preliminary estimate of the “background level”  $A$ . After that, all the points above  $A$  have been involved in the final treatment.

The models  $F^1$  and  $F^3$  fit the data equally well. Let us discuss the model  $F^2$  and the role of the second correction. As



**Table 1.** Model parameters and their central 0.95 confidence intervals as the results of light curve fitting for Q2237+0305C. The data due to OGLE group (Wozniak et al. 2000).

Fitting model	$t_C$ (JD-2450000)	$T$ (days)	$A$ (mJy)	$B$ (mJy)	Correction coefficient (mJy)	$S_{min}$	$\nu$	$\chi^2$
$F^0$	$1384.7^{+1.0}_{-1.0}$	$33.0^{+2.7}_{-2.6}$	$0.364^{+0.006}_{-0.006}$	$0.076^{+0.003}_{-0.003}$		53.91	40	1.35
$F^1$	$1382.6^{+1.5}_{-1.7}$	$34.7^{+2.9}_{-2.7}$	$0.366^{+0.006}_{-0.006}$	$0.079^{+0.004}_{-0.004}$	$C = -0.006^{+0.003}_{-0.004}$	38.43	39	0.99
$F^2$	$1367.1^{+4.4}_{-3.4}$	$40.1^{+3.2}_{-3.5}$	$0.363^{+0.006}_{-0.007}$	$0.067^{+0.005}_{-0.004}$	$D = -0.071^{+0.014}_{-0.010}$	34.97	39	0.90
$F^3$	$1383.3^{+1.3}_{-1.4}$	$34.9^{+3.2}_{-2.6}$	$0.358^{+0.007}_{-0.008}$	$0.080^{+0.005}_{-0.004}$	$E = -0.004^{+0.002}_{-0.003}$	39.38	39	1.01

Notation for the fitting models and the parameters are given in the text.

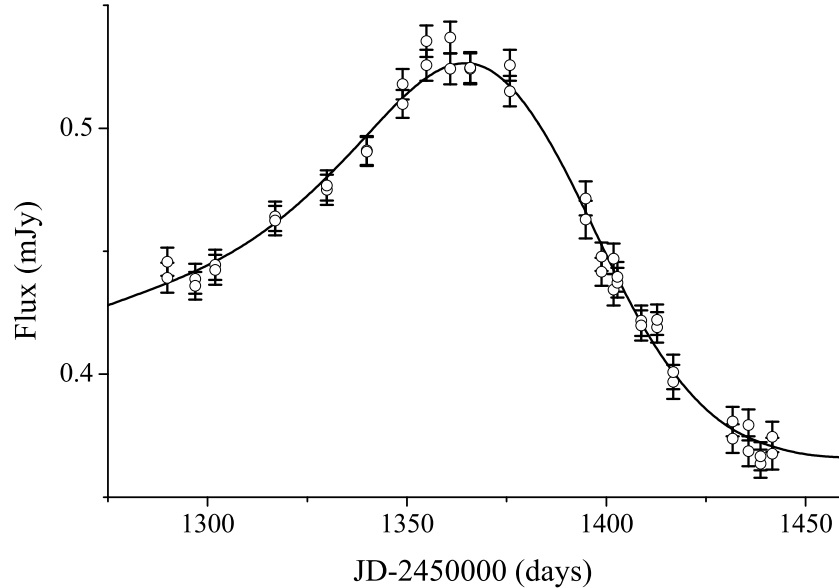


**Figure 3.** Observed light curve of Q2237+0305C (OGLE data) and the best-fitting with the model  $F^1$  (solid line).

compared with the other models, the model  $F^2$  leads to a somewhat lower value of  $\chi^2$ , but the confidence interval for  $t_C$  is four times wider than that in the case of the model  $F^0$ , and the source size appears to be 20 per cent more than that within other models. Here, the typical features of the second correction mentioned in the previous section become apparent. The true determination of  $D$  from formula (28) could allow us to estimate the ratio of the curvature and source radii:  $\kappa L = -2D/B$ . But the obtained value of  $D$  corresponds to the curvature radius  $R_c \equiv 1/\kappa$  that is about twice less than the source “size”  $L$ . So, the condition of smallness of the correction is violated, and the model  $F^2$  is not acceptable. On the other hand, neglecting the second correction in (28) (i.e., the transition to the model  $F^1$ ) corresponds to  $R_c \gg L$ . Our calculations have shown that the *a priori* assignment  $R_c > L$  and the introduction of the appropriate additional term into the model  $F^1$  have little influence on the estimates of  $A$ ,  $B$ , and  $C$ .

To sum up, the model  $F^1$  fits satisfactorily the data on HAE in question within the present accuracy, though we cannot rule out competing models and/or competing effects.

We also analysed HAE in the light curve of image Q2237+0305A that happened in 1999 (Wozniak et al. 2000). However, the treatment of this HAE does not allowed us to find statistically significant estimates of the corrections because of lacking the data corresponding to the caustic inner region.

## 6 DISCUSSION

We proposed two methods that enabled us to obtain the critical solutions of the gravitational lens equation near a fold caustic with any desired accuracy. The first method is based on the expansion of the solutions and the amplification factor  $K_{cr}$  of two critical images of a point source in powers of a formal parameter  $t$  that can be interpreted as a parameter describing the

proximity to the caustic. We derived a representation of  $K_{cr}$  which is convenient to obtain the amplification factor for an extended source. This representation is not analytic in local coordinates, and  $K_{cr}$  contains a nonintegrable term. In order to elucidate this term, we considered a different representation of the solutions which contains analytic functions of coordinates and the parameter  $t$ , as well as square roots of such functions. This method yields only integrable expressions and explains the meaning of the nonintegrable term in  $K_{cr}$ : it should be considered as a distribution which can be used to calculate the amplification of a small (and smooth) extended source near the fold caustic by taking the appropriate convolution.

In order to obtain nontrivial corrections to  $K_{cr}$ , we had to use higher orders of the expansion of the lens equation as compared to works by Alexandrov et al. (2003) and Keeton et al. (2005). This is a consequence of the cancellation of terms  $\sim O(t^2)$  which are present in the amplifications of separate critical images. Therefore, we had to deal with terms of the order  $\sim O(t^3)$  and the Taylor expansion including the 4-th order in the lens equation (3). The modified formula for  $K_{cr}$  contains 3 extra parameters that are combinations of 5 coefficients of the Taylor expansion (we confined ourselves to the case of no continuous matter on the line of sight).

Based on our result concerning  $K_{cr}$ , we derived an asymptotic formula for the amplification  $K_G$  of a small Gaussian source. We analysed the role of new “post-linear” corrections and formulated the conditions of applicability of the linear caustic approximation. The fitting of the light curve of GLS Q2237+0305C shows that some of these corrections can be statistically significant.

Of course, we are far from the thought that the available observational data make it possible to determine all additional parameters simultaneously (and even more so, the coefficients of the expansion of the lens mapping up to the orders involved). Such a determination requires a considerable improvement of the photometric accuracy in the future. Our result is more modest: we have shown that, even at the present level of accuracy, some elements of the light curves require to consider the higher-order terms in the solutions of the lens equation. At least, after the introduction of some post-linear corrections,  $\chi^2$  decreases by 30 per cent thus approaching 1. One may hope that an enhancement of the observational accuracy will increase the role of post-linear approximations.

In this connection, we note that, besides estimating the source size in GLS on the basis of light curves, a number of authors (Shalyapin 2001; Shalyapin et al. 2002; Bogdanov & Cherepashchuk 2002; Goicoechea et al. 2003; Kochanek 2004; Mortonson et al. 2005; Gil-Merino et al. 2006; Vakulik et al. 2007; Anguita et al. 2008) discussed some delicate questions concerning a fine quasar structure. For example, Goicoechea et al. (2003) wrote that the GLITP data (Alcalde et al. 2002) on GLS Q2237+0305 admit only accretion disc models (see also Gil-Merino et al. 2006; Anguita et al. 2008). Obviously, the presence of an accretion disk in a central region of quasar is beyond any doubts, as well as the fact that the real appearance of the quasar core can be quite different from very simplified theoretical models in question. On the other hand, Mortonson et al. (2005) argue that the accretion disk can be modelled with any brightness profile (Gaussian, uniform, etc.), and this model will agree with the available data provided that an appropriate source size is chosen. Anyway, in these considerations, different effects come into play, and the consistent treatment requires to consider all the corrections to the amplification including those obtained in the present paper.

## ACKNOWLEDGMENTS

This work has been supported in part by the “Cosmomicrophysics” programme of the National Academy of Sciences of Ukraine. VIZ also acknowledges the partial support of Swiss National Science Foundation (SCOPES grant 128040). We would also like to thank anonymous referees for stimulating comments that helped us to improve the text and initiated the writing of Appendices C and D.

## REFERENCES

- Alcalde D. et al., 2002, *ApJ*, **572**, 729  
 Alexandrov A.N., Zhdanov V.I., Fedorova E.V., 2003, *Visnyk Kyivskogo Universytetu, Astronomiya* (in Ukrainian), **39-40**, 52  
 Anguita T., Schmidt R.W., Turner E.L., Wambsganss J., Webster R.L., Loomis K.A., Long D., MacMillan R., 2008, *A&A*, **480**, 327  
 Bateman H., Erdélyi A., 1953, *Higher Transcendental Functions, Vol. 1* (New York: Mc Graw-Hill)  
 Bogdanov M.B., Cherepashchuk A.M., 2002, *Astronomy Repts.*, **46**, 626  
 Cassan A., 2008, *A&A*, **491**, 587  
 Congdon A.B., Keeton C.R., Nordgren C.E., 2008, *MNRAS*, **389**, 398  
 Dai X., Agol E., Bautz M.W., Garmire G.P., 2003, *ApJ*, **589**, 100  
 Dominik M., 2004, *MNRAS*, **353**, 69  
 Fedorova E.V., Zhdanov V.I., Vignali C., Palumbo G.G.C., 2008, *A&A*, **490**, 989

- Fluke C.J., Webster R.L., 1999, MNRAS, **302**, 68  
 Gaudi B.S., Petters A.O., 2002, ApJ, **574**, 970  
 Gel'fand I.M., Shilov G.E., 1964, *Generalized Functions, Vol. 1* (New York: Academic Press)  
 Gil-Merino R., Gonzalez-Cadelo J., Goicoechea L.J., Shalyapin V.N., Lewis G.F., 2006, MNRAS, **371**, 1478  
 Goicoechea L.J., Alcalde D., Mediavilla E., Muñoz J.A., 2003, A&A, **397**, 517  
 Grieger B., Kayser R., Refsdal S., 1988, A&A, **194**, 54  
 Huchra J., Gorenstein V., Kent S., Shapiro I., Smith G., Horine E., Perley R., 1985, AJ, **90**, 691  
 Keeton C.R., Gaudi B.S., Petters A.O., 2005, ApJ, **635**, 35  
 Kochanek C.S., 2004, ApJ, **605**, 58  
 Moreau O., Libbrecht C., Lee D.-W., Surdej J., 2005, A&A, **436**, 479  
 Mortonson M.J., Schechter P.L., Wambsganss J., 2005, ApJ, **628**, 594  
 Pejcha O., Heyrovský D., 2009, ApJ, **690**, 1772  
 Petters A.O., Levine H., Wambsganss J., 2001, *Singularity Theory and Gravitational Lensing* (Boston: Birkhäuser)  
 Poindexter S., Kochanek C.S., 2010a, ApJ, **712**, 658  
 Poindexter S., Kochanek C.S., 2010b, ApJ, **712**, 668  
 Poindexter S., Morgan N., Kochanek C.S., 2008, ApJ, **673**, 34  
 Poston T., Stewart I., 1978, *Catastrophe Theory and Its Applications* (London: Pitman)  
 Schmidt R., Webster R.L., Lewis F.G., 1998, MNRAS, **295**, 488  
 Schneider P., Ehlers J., Falco E.E., 1992, *Gravitational Lenses* (New York: Springer)  
 Schneider P., Weiß A., 1987, A&A, **171**, 49  
 Shalyapin V.N., 2001, Astronomy Lett., **27**, 150  
 Shalyapin V.N., Goicoechea L.J., Alcalde D., Mediavilla E., Muñoz J.A., Gil-Merino R., 2002, ApJ, **579**, 127  
 Udalski A., et al., 2006, Acta Astron. **56**, 293  
 Vakulik V., Schild R., Dudinov V., Nuritdinov S., Tsvetkova V., Burkhonov O., Akhunov T., 2006, A&A, **447**, 905  
 Vakulik V.G., Schild R.E., Smirnov G.V., Dudinov V.N., Tsvetkova V.S., 2007, MNRAS, **382**, 819  
 Wambsganss J. 2006, in: Kochanek C.S., Schneider P., Wambsganss J. *Gravitational Lensing: Strong, Weak and Micro*.  
 Editors: G. Meylan, P. Jetzer, P. North (Berlin: Springer-Verlag)  
 Wozniak P.R., Alard C., Udalski A., Szymański M., Kubiak M., Pietrzyński G., Zebruń K., 2000, ApJ, **529**, 88  
 Wyithe J.S., Webster R.L., Turner E.L., 1999, MNRAS, **309**, 261  
 Wyithe J.S., Webster R.L., Turner E.L., 2000, MNRAS, **318**, 762  
 Wyithe J.S., Webster R.L., Turner E.L., Mortlock D.J., 2000, MNRAS, **315**, 62  
 Yonehara A., 2001, AJ, **548**, L127

## APPENDIX A: ANALYTICAL EXPANSION METHOD

Here, we present a justification of the method of analytical expansions near the folds used in Section 3.1 following Alexandrov et al. (2003). This problem is not trivial, because the Jacobian of the lens mapping on the fold is equal to zero.

We say that an analytic function  $f(t)$  has order  $k$  at  $t = 0$ , if  $f^{(i)}(0) = 0$  for  $i = 0, 1, \dots, k - 1$ , and  $f^{(k)}(0) \neq 0$  (Poston & Stewart 1978); then we write  $f(t) = O(t^k)$ .

It is well known that the mapping

$$\mathbf{y} = \mathbf{F}(\mathbf{x}) \tag{A1}$$

of two-dimensional manifolds (e.g., mapping (3)) in a neighborhood of the fold ( $\mathbf{x} = \mathbf{y} = 0$ ) can be reduced by the coordinate transformations

$$\mathbf{u} = \mathbf{u}(\mathbf{x}), \quad \mathbf{v} = \mathbf{v}(\mathbf{y}), \quad \mathbf{x} = \mathbf{x}(\mathbf{u}), \quad \mathbf{y} = \mathbf{y}(\mathbf{v}) \tag{A2}$$

to the normal form (see, e.g., Poston & Stewart 1978; Petters et al. 2001):

$$\mathbf{u} \rightarrow \mathbf{v} : \quad v_1 = u_1, \quad v_2 = (u_2)^2. \tag{A3}$$

We suppose the initial mapping (A1) is analytic; then transformations (A2) are also analytic.

Let the source move along a parameterized curve  $\mathbf{v}(t)$  such that (i)  $v_2(t) > 0$  for  $t \neq 0$ ,  $\mathbf{v}(0) = 0$ ; (ii) the functions  $v_i(t)$  are analytic at  $t = 0$ ; (iii) the order of  $v_2(t)$  is  $2k$  for some integer  $k \geq 1$ . Conditions (ii) and (iii) mean that  $v_2(t) = t^{2k}(q + \chi(t))$ ,  $q \neq 0$ , and  $\chi(t)$  is analytic function at  $t = 0$  so that  $\chi(0) = 0$ . In view of (i), we have  $q + \chi(t) > 0$ .

We have two obvious solutions of Eqs. (A3):

$$\mathbf{u}_{(\pm)}(t) = \{v_1(t), \pm t^k \sqrt{q + \chi(t)}\}, \tag{A4}$$

which, in view of  $q > 0$ , are analytic as functions of  $t$  at the common point  $t = 0$ . We can say that the trajectory of the source consists of two branches, corresponding to values  $t < 0$  and  $t > 0$ . Each branch has two images lying on different sides of the critical curve. When  $k$  is even (odd), the images which lie on the one side (on different sides) continue analytically one another. Thus, a suitable choice of the source trajectory  $\mathbf{v}(t)$  leads to the analyticity of its critical images as functions of the parameter.

We now intend to reformulate the sufficient conditions of the existence of analytical solutions in the original coordinates. The coordinate transformation  $\mathbf{y} \rightarrow \mathbf{v}$  in the source plane can be written as

$$v_1 = Ay_1 + By_2 + \Phi_1(y_1, y_2), \quad (\text{A5})$$

$$v_2 = Cy_1 + Dy_2 + \Phi_2(y_1, y_2), \quad (\text{A6})$$

$$AD - BC \neq 0.$$

Here,  $\Phi_i(y_1, y_2)$  are analytic functions having the Taylor expansions starting from the second order.

Then we assume that the terms linear in  $x_i$  are present only in the first component,  $F_1(\mathbf{x})$ , of the lens mapping (A1). Then, in Eq. (A6),  $C = 0$ . This statement follows from the substitution of (A1) in (A6), the application of the transformation  $\mathbf{x} = \mathbf{x}(\mathbf{u})$ , and the comparison with the second equation in (A3).

Suppose that

(a) the curve  $\mathbf{y}(t)$  lies on the inner side of the caustic (except  $\mathbf{y}(0) = 0$ ),

(b)  $\mathbf{y}(t)$  is analytic and such that  $y_1(t) = O(t^m)$ ,  $y_2(t) = O(t^{2k})$ ;  $m > k \geq 1$ , and  $m$  and  $k$  are integers.

Then Eq. (A6) yields  $v_2(t) = O(t^{2k})$  and conditions (i), (ii), and (iii) are fulfilled.

In summary, we obtain the following statement.

Let the function  $\mathbf{F}(\mathbf{x})$  of the lens equation (A1) be an analytic function of  $\mathbf{x}$  in a neighborhood of the fold critical point  $\mathbf{x} = 0$ , let  $\mathbf{y} = 0$  be the corresponding caustic point, and let  $F_2(\mathbf{x})$  do not contain linear terms. Let also  $\mathbf{y}(t)$  be an analytic vector-function which represents the curve satisfying conditions (a), (b).

Then the lens equation A1 has two solutions  $\mathbf{x}_{(+)}(t)$  and  $\mathbf{x}_{(-)}(t)$  which are analytic in  $t$  and represent the critical images of the curve  $\mathbf{y}(t)$ .

These conditions are sufficient ones, and they do not exhaust possible combinations of  $k, m$ . Typically, the statement is true also when  $m = k$ . This statement allows us to use analytical expansions along test source trajectories to obtain the critical solutions near the folds. In the main body of this paper, we have used the family of straight-line trajectories of the source  $y_i(t) = a_i t^2$  ( $k = 1, m = 2$ ) in a neighborhood of the caustic on one side from the tangent to the caustic. In work (Alexandrov et al. 2003), we also considered the version with parabolic curves  $y_1(t) = at$ ,  $y_2(t) = bt^2$ , which allowed us to find the solutions in the approximation of a parabolic caustic.

## APPENDIX B: ANALYTICAL ITERATION METHOD

In this Appendix, we show that the critical solutions of the lens equation (3) (after the substitution of (4)) can be represented in the form (11), the functions  $p, r, \bar{s}, w$  being polynomials in  $t, y_1$ , and  $y_2$  on every step of the approximation procedure.

Here, we use the notations which are independent of the rest of the paper. After a simple change of the variables ( $y_1 = (b\tilde{y}_1 - a\tilde{y}_2)/2b$ ,  $y_2 = -\tilde{y}_2/b$ ), Eq. (6) can be written in the form

$$\begin{aligned} y_1 &= x_1 + t \sum_{n,m} a_{n,m}(t) x_1^n x_2^m, \\ y_2 &= x_2^2 + t \sum_{n,m} b_{n,m}(t) x_1^n x_2^m, \end{aligned} \quad (\text{B1})$$

where the indices  $m, n$  take on integer nonnegative values;  $t$  is a small parameter; the coefficients  $a_{n,m}(t)$  and  $b_{n,m}(t)$  are finite-order polynomials in  $t$ . In fact, all considerations below can be performed in the case where the r.h.s. of (B1) is an analytic functions in  $x_1, x_2$ , and the small parameter  $t$ . However, in this paper, we deal with finite-order approximations.

We search for a solution in the form

$$x_1 = p + t\varepsilon r\sqrt{w}, \quad x_2 = ts + \varepsilon\sqrt{w}; \quad \varepsilon = \pm 1. \quad (\text{B2})$$

After the substitution of Eq. (B2) in (B1), we separate the terms containing integer and half-integer powers of  $w$ , e.g.,

$$\sum_{n,m} a_{n,m}(p + \varepsilon tr\sqrt{w})^n (ts + \varepsilon\sqrt{w})^m = A_0 + \varepsilon w^{1/2} A_1,$$

where

$$\begin{aligned}
 A_0 &= \sum_{n,m} a_{n,m} \sum_{\substack{k,k' \\ k+k'=2K}} C_n^k C_m^{k'} (tr)^k p^{n-k} (ts)^{m-k'} w^K, \quad K = \frac{k+k'}{2} \text{ is an integer,} \\
 A_1 &= \sum_{n,m} a_{n,m} \sum_{\substack{k,k' \\ k+k'=2\bar{K}+1}} C_n^k C_m^{k'} (tr)^k p^{n-k} (ts)^{m-k'} w^{\bar{K}}, \quad \bar{K} = \frac{k+k'-1}{2} \text{ is an integer.}
 \end{aligned} \tag{B3}$$

Here,  $C_n^k$  are the binomial coefficients,  $C_n^k = 0$  for  $k > n$  and for  $k < 0$ ; and  $k, k'$  are nonnegative integers.

Then we equate separately the terms with integer and half-integer powers of  $w$  on both sides of the relation following from the first equation of system (B1) and obtain

$$p = y_1 + tP(t, p, r, s, w), \tag{B4}$$

where

$$P(t, p, r, s, w) \equiv -A_0,$$

and

$$r + A_1 = 0. \tag{B5}$$

Analogously, the second equation of (B1) yields

$$w = y_2 + tW(t, p, r, s, w), \tag{B6}$$

where

$$W(t, p, r, s, w) \equiv -ts^2 - B_0,$$

and

$$2s + B_1 = 0. \tag{B7}$$

Here,  $B_0$  and  $B_1$  are defined similarly to  $A_0$  and  $A_1$  by Eq. (B3) with the replacement of the coefficients,  $a_{n,m} \rightarrow b_{n,m}$ .

Separating the terms of the zero order with respect to  $r$  and  $s$  (or with respect to  $t$ ) in Eq. (B3), we rewrite Eq. (B5) as follows:

$$r + \sum_{n,K} a_{n,2K+1} p^n w^K + tU(t, p, r, s, w) = 0. \tag{B8}$$

Here,

$$U(t, p, r, s, w) \equiv \sum_{n,m} a_{n,m} \sum_{\substack{k,k' \\ k+k'=2K+1 \\ k+m-k'>0}} C_n^k C_m^{k'} t^{k+m-k'-1} r^k p^{n-k} s^{m-k'} w^K.$$

Substituting  $p$  and  $w$  from Eqs. (B4) and (B6) in Eq. (B8), we get

$$r + \sum_{n,K} a_{n,2K+1} (y_1 + tP)^n (y_2 + tW)^K + tU(t, p, r, s, w) = 0.$$

This relation can be written as

$$r = f(t, y_1, y_2) + tR(t, p, r, s, w), \tag{B9}$$

where

$$f(t, y_1, y_2) \equiv - \sum_{n,K} a_{n,2K+1} y_1^n y_2^K,$$

$$R(t, p, r, s, w) \equiv - \sum_{n,K} a_{n,2K+1} \sum_{\substack{k,k' \\ k+k'>0}} C_n^k C_K^{k'} y_1^{n-k} y_2^{K-k'} P^k W^{k'} t^{k+k'-1} - U(t, p, r, s, w).$$

An analogous consideration of Eq. (B7) yields

$$s + \frac{1}{2} \sum_{n,K} b_{n,2K+1} p^n w^K + \frac{t}{2} V(t, p, r, s, w) = 0,$$

where

$$V(t, p, r, s, w) \equiv \sum_{n,m} b_{n,m} \sum_{\substack{k,k' \\ k+k'=2K+1 \\ k+m-k'>0}} C_n^k C_m^{k'} t^{k+m-k'-1} r^k p^{n-k} s^{m-k'} w^K.$$

Then we substitute  $p$  and  $w$  from Eqs. (B4) and (B6) to obtain

$$s = g(t, y_1, y_2) + tS(t, p, r, s, w), \quad (\text{B10})$$

where

$$g(t, y_1, y_2) \equiv -\frac{1}{2} \sum_{n,K} b_{n,2K+1} y_1^n y_2^K,$$

$$S(t, p, r, s, w) \equiv -\frac{1}{2} \left[ \sum_{n,K} b_{n,2K+1} \sum_{\substack{k,k' \\ k+k'>0}} C_n^k C_K^{k'} y_1^{n-k} y_2^{K-k'} P^k W^{k'} t^{k+k'-1} + V(t, p, r, s, w) \right].$$

Thus, we have the system of equations (B4), (B9), (B10), (B6) for  $p, r, s,$  and  $w$  that can be represented in the form

$$\mathbf{X} = \mathbf{F}(t, \mathbf{Y}) + t\mathbf{G}(t, \mathbf{X}, \mathbf{Y}), \quad (\text{B11})$$

where

$$\mathbf{X} = \begin{Bmatrix} p \\ r \\ s \\ w \end{Bmatrix}, \quad \mathbf{Y} = \begin{Bmatrix} y_1 \\ y_2 \end{Bmatrix}, \quad \mathbf{F}(t, \mathbf{Y}) = \begin{Bmatrix} y_1 \\ f(t, y_1, y_2) \\ g(t, y_1, y_2) \\ y_2 \end{Bmatrix}, \quad \mathbf{G}(t, \mathbf{X}, \mathbf{Y}) = \begin{Bmatrix} P(t, p, r, s, w) \\ R(t, p, r, s, w) \\ S(t, p, r, s, w) \\ W(t, p, r, s, w) \end{Bmatrix}.$$

System (B11) is ready for iterations

$$\mathbf{X}_{(n)} = \mathbf{F}(t, \mathbf{Y}) + t\mathbf{G}(t, \mathbf{X}_{(n-1)}, \mathbf{Y}), \quad n = 1, 2, \dots, \quad \mathbf{X}_{(0)} = \mathbf{F}(t, \mathbf{Y}).$$

For a sufficiently small  $t$ , the iteration process converges due to the contraction mapping theorem. It is worth to note that, at every iteration step, we obtain an approximate solution in the form of finite-order polynomials in  $\mathbf{Y}$ . This is obvious from the explicit form of the functions  $f(t, y_1, y_2), g(t, y_1, y_2), P(t, p, r, s, w), R(t, p, r, s, w), S(t, p, r, s, w),$  and  $W(t, p, r, s, w)$ . The application of the above procedure to system (6) yields solution (11-14).

### APPENDIX C: AMPLIFICATION FOR A POWER-LAW SOURCE

Here, we use Eq. (18) to derive the magnification of an extended centrally symmetric source with a power-law brightness distribution. Two different types of ‘‘power-law’’ distributions can be found in the literature on the gravitational lensing. In particular, there are the distributions (Shalyapin 2001; Shalyapin et al. 2002)

$$I_p^{(-)}(\mathbf{y}) = \frac{p-1}{\pi L^2} [1 + \mathbf{y}^2/L^2]^{-p}, \quad (\text{C1})$$

where  $p > 1$  is the power index, the source centre is at the coordinate origin, the distribution (C1) is normalized to unity, and  $L$  is related to the r.m.s. radius  $R_{rms}$  as  $L^2 = (p-2) R_{rms}^2$ ,

$$R_{rms}^2 = \int dy_1 dy_2 \mathbf{y}^2 I_p^{(-)}(\mathbf{y}).$$

For fixed  $R_{rms}$  and  $p \rightarrow \infty$ , the brightness distribution (C1) tends to the Gaussian one.

Along with (C1), the models for limb darkening are also often used in microlensing studies (see, e.g., Dominik 2004)

$$I_q^{(+)}(\mathbf{y}) = \frac{q+1}{\pi L^2} \Xi(|\mathbf{y}|/L; q), \quad \Xi(\xi; q) = \Theta(1 - \xi^2)(1 - \xi^2)^q, \quad (\text{C2})$$

where  $L$  stands for the source radius, and  $L^2 = (q+2) R_{rms}^2$ . Here, we assume  $q > 0$ . Linear combinations of distributions (20), (C1), and (C2) with different parameters yield rather a wide class of symmetric source models.

For brightness profile (C1), the total microlensed flux (18) that describes a variable contribution of the critical images, as the source crosses a fold caustic, is the convolution of (C1) with (19). The result for the amplification factor involves integrals that can be expressed via the hypergeometric function  ${}_2F_1$  (Bateman & Erdélyi 1953):

$$\Psi_{k,p}(h) = \frac{\Gamma(p - \frac{1}{2})}{\Gamma(p - 1)} \int_0^\infty \frac{y^{k-\frac{1}{2}} dy}{(1 + (y-h)^2)^{p-1/2}} =$$

$$= \frac{\Gamma\left(p - \frac{1}{2}\right)}{\Gamma(p-1)} B\left(k + \frac{1}{2}, 2p - k - \frac{3}{2}\right) (1 + h^2)^{k/2+3/4-p} {}_2F_1\left(k + \frac{1}{2}, 2p - k - \frac{3}{2}; p; \frac{1}{2} \left(1 + \frac{h}{\sqrt{1+h^2}}\right)\right) \quad (\text{C3})$$

for  $k = 0, 1$ ,  $B(x, y)$  being the Beta-function.

We extend (C3) to  $k = -1$  having in mind the definition of  $(y)_+^{-3/2}$ , so that

$$\Psi_{-1,p}(h) = 4(p-1)[h\Psi_{0,p+1}(h) - \Psi_{1,p+1}(h)]. \quad (\text{C4})$$

Like in Subsection 4.3, we introduce the normalized coordinates of the source center  $s = Y_1/L$ ,  $h = Y_2/L$ . Now, the amplification due to critical images takes on the form

$$K_p^-(s, h) = \frac{1}{2\sqrt{\pi|b|L}} \left\{ \Psi_{0,p}(h) + L \left[ P\Psi_{1,p}(h) - \frac{\kappa}{8(p-2)}\Psi_{-1,p-1}(h) + Qs\Psi_{0,p}(h) - \frac{\kappa}{4}s^2\Psi_{-1,p}(h) \right] \right\}. \quad (\text{C5})$$

The zeroth approximation to this formula has been derived by Shalyapin (2001).

In the case of the model with limb darkening (C2), the critical images disappear when the source lies on the outer side of the caustic (i.e., for  $h < -1$ ). The substitution of (C2) and (19) in (18) yields the total amplification of critical images as

$$K_q^{(+)}(s, h) = \frac{1}{2\sqrt{\pi|b|L}} \left\{ X_{0,q}(h) + L \left[ PX_{1,q}(h) - \frac{\kappa}{8(q+2)}X_{-1,q+1}(h) + QsX_{0,q}(h) - \frac{\kappa}{4}s^2X_{-1,q}(h) \right] \right\}, \quad (\text{C6})$$

where we denote

$$X_{k,q}(h) = \frac{\Gamma(q+2)}{\Gamma\left(q + \frac{3}{2}\right)} \int_0^\infty y^{k-\frac{1}{2}} \Xi(y-h; q+1/2) dy, \quad k = 1, 2.$$

Like the previous analogous cases, we define

$$X_{-1,q}(h) = 4(q+1)(hX_{0,q-1} - X_{1,q-1}).$$

We have

$$X_{k,q}(h) = 2^{q+\frac{1}{2}}(1+h)^{q+k+1} \frac{\Gamma(q+2)\Gamma\left(k + \frac{1}{2}\right)}{\Gamma(q+k+2)} {}_2F_1\left(-q - \frac{1}{2}, q + \frac{3}{2}; q+k+2; \frac{1+h}{2}\right),$$

for  $-1 < h < 1$  and

$$X_{k,q}(h) = \sqrt{\pi}(h+1)^{k-\frac{1}{2}} {}_2F_1\left(q + \frac{3}{2}, \frac{1}{2} - k; 2q+3; \frac{2}{h+1}\right),$$

for  $h > 1$ .

The functions  $\Psi_{0,p}$ ,  $\Psi_{1,p}$ ,  $\Psi_{-1,p}$ , and  $X_{0,q}$ ,  $X_{1,q}$ ,  $X_{-1,q}$  are analogous to  $\Phi_0$ ,  $\Phi_1$ ,  $4\Phi_2$  from (25), respectively; they have a similar qualitative behavior and the same asymptotics. Note that all formulas for the extended source models are transformed into that for point-source amplification (19), as the source size tends to zero.

#### APPENDIX D: EXPLICIT COMPARISON OF THE FIRST-ORDER FORMULAS WITH COUNTERPARTS FROM THE PAPER BY KEETON, GAUDI & PETERS (2005)

Here we compare our expressions for the first order corrections with that of Appendix A2 from (Keeton et al. 2005), further KGP. This is especially relevant because KGP considers the general case of the lens equation without supposition on harmonic potential.

Initial equations (A7-A8) of the lens mapping of KGP are as follows

$$\xi u_1 = K\theta_1 - (3e\theta_1^2 + 2f\theta_1\theta_2 + g\theta_2^2) - (4k\theta_1^3 + 3m\theta_1^2\theta_2 + 2n\theta_1\theta_2^2 + p\theta_2^3),$$

$$\xi u_2 = - (f\theta_1^2 + 2g\theta_1\theta_2 + 3h\theta_2^2) - (m\theta_1^3 + 2n\theta_1^2\theta_2 + 3p\theta_1\theta_2^2 + 4r\theta_2^3).$$

These equations need to be compared to our Eqs. (3-6). The correspondence between the coordinate notations is  $\theta_i \leftrightarrow x_i$ ,  $u_i \leftrightarrow \tilde{y}_i$ ,  $\xi \leftrightarrow t^2$ .

In the general case the lens potential  $\Phi(\mathbf{x})$  obeys the equation

$$\Delta\Phi = 2\sigma(\mathbf{x}), \quad (\text{D1})$$

where  $\sigma(\mathbf{x})$  is the normalized surface density of the continuous matter. Coordinates are chosen to diagonalize the symmetric matrix  $A_{ij} = \partial y_i / \partial x_j|_{\mathbf{x}=0}$ . Its eigenvalues are  $\lambda_1 = 1 - \sigma(0) + \Gamma(0)$  and  $\lambda_2 = 1 - \sigma(0) - \Gamma(0)$ , where  $\Gamma$  is modulus of the complex shear (see, e.g., Schneider et al. 1992). At the critical point one of the eigenvalues is zero (the coordinates are chosen so that  $\partial y_2 / \partial x_2|_{\mathbf{x}=0} = 0$ ), in this case we have  $\partial y_1 / \partial x_1|_{\mathbf{x}=0} = K = 2[1 - \sigma(0)]$ .

Now we consider the correspondence of the expansion coefficients. For example Eq. (1) yields  $3e = \frac{1}{2}\Phi_{,111}$ ;  $g = \frac{1}{2}\Phi_{,122}$ . Under the assumption that during HAE  $\sigma = \sigma_0 = \text{const}$  we have  $3e = -g \rightarrow -a$ . Analogously  $f = -3h \rightarrow -b$ ,  $4k = -\frac{2}{3}n = 4r \rightarrow -c$ ,  $p = -m \rightarrow d$ .

For critical solutions near a fold caustic, KGP found Eqs. (A14-A15) which we repeat below along with our analogs

$$\begin{aligned} \theta_1^\pm &= \frac{3hu_1 - gu_2}{3hK} \xi + O(\xi)^{3/2} \rightarrow x_1 = \tilde{x}_1 t^2 = \frac{b\tilde{y}_1 - a\tilde{y}_2}{2b(1-\sigma_0)} t^2 + O(t^3), \\ \theta_2^\pm &= \mp \sqrt{\frac{-u_2}{3h}} \xi^{1/2} - \frac{3ghu_1 - (g^2 + 2Kr)u_2}{9h^2K} \xi + O(\xi)^{3/2} \rightarrow \\ x_2 = \tilde{x}_2 t &= -\varepsilon \sqrt{\frac{-\tilde{y}_2}{b}} t - \frac{ab\tilde{y}_1 - [a^2 - c(1-\sigma_0)]\tilde{y}_2}{2b^2(1-\sigma_0)} t^2 + O(t^3). \end{aligned} \quad (\text{D2})$$

For  $\sigma_0 = 0$  these expressions are equivalent to  $\tilde{x}_1 = \tilde{x}_{10} + O(t)$ ,  $\tilde{x}_2 = \tilde{x}_{20} + \tilde{x}_{21}t + O(t^2)$ , where  $\tilde{x}_{10}, \tilde{x}_{20}, \tilde{x}_{21}$  are given by (7-8). Thus (from the viewpoint of our approach) KGP derives the first coordinate in zero approximation. However, as KGP point out this is sufficient to find the first order correction for the amplification. Namely, for the corresponding Jacobian of the lens mapping, KGP found (A17):

$$\begin{aligned} (\mu^\pm)^{-1} &= \pm 2K \sqrt{-3hu_2\xi}^{1/2} + \frac{4}{3h} (g^2 - 3fh + 2Kr) u_2 \xi + O(\xi)^{3/2} \rightarrow \\ J &= 4\varepsilon t (1 - \sigma_0) \sqrt{-b\tilde{y}_2} + \frac{4}{b} t^2 [a^2 + b^2 - c(1 - \sigma_0)] \tilde{y}_2 + O(t^3). \end{aligned} \quad (\text{D3})$$

For  $\sigma_0 = 0$  the latter equation is the same (in the first approximation) as Eq.(15).

For  $\sigma_0 \neq 0$  the approximate solutions follow from the corresponding ones with  $\sigma_0 = 0$  by means of the rescaling

$$\tilde{y}_i \rightarrow \tilde{y}_i / (1 - \sigma_0), \quad a \rightarrow a / (1 - \sigma_0), \quad b \rightarrow b / (1 - \sigma_0), \quad c \rightarrow c / (1 - \sigma_0), \quad \dots \quad (\text{D4})$$

Analogous rescaling for the Jacobian is  $J \rightarrow J(1 - \sigma_0)^2$ ; it is this rescaling of the variables has been mentioned in Section 2.